JACS
JOURNAL OF THE AMERICAN CHEMICAL SOCIETY

pubs.acs.org/JACS

Article

It is Better with Salt: Aqueous Ring-Opening Metathesis Polymerization at Neutral pH

Jeffrey C. Foster,*[,†] Marcus C. Grocott,[†] Lucy A. Arkinstall, Spyridon Varlas, McKenna J. Redding, Scott M. Grayson,* and Rachel K. O'Reilly*

Cite This: *J. Am. Chem. Soc.* 2020, 142, 13878–13885

Read Online

ACCESS | Metrics & More | Article Recommendations | Supporting Information

ABSTRACT: Aqueous ring-opening metathesis polymerization (ROMP) is a powerful tool for polymer synthesis under environmentally friendly conditions, functionalization of biomacromolecules, and preparation of polymeric nanoparticles via ROMP-induced self-assembly (ROMPISA). Although new water-soluble Ru-based metathesis catalysts have been developed and evaluated for their efficiency in mediating cross metathesis (CM) and ring-closing metathesis (RCM) reactions, little is known with regards to their catalytic activity and stability during aqueous ROMP. Here, we investigate the influence of solution pH, the presence of salt additives, and catalyst loading on ROMP monomer conversion and catalyst lifetime. We find that ROMP in aqueous media is particularly sensitive to chloride ion concentration and propose that this sensitivity originates from chloride ligand displacement by hydroxide or H_2O at the Ru center, which reversibly generates an unstable and metathesis inactive complex. The formation of this Ru-$(OH)_n$ complex not only reduces monomer conversion and catalyst lifetime but also influences polymer microstructure. However, we find that the addition of chloride salts dramatically improves ROMP conversion and control. By carrying out aqueous ROMP in the presence of various chloride sources such as NaCl, KCl, or tetrabutylammonium chloride, we show that diblock copolymers can be readily synthesized via ROMPISA in solutions with high concentrations of neutral H_2O (i.e., 90 v/v%) and relatively low concentrations of catalyst (i.e., 1 mol %). The capability to conduct aqueous ROMP at neutral pH is anticipated to enable new research avenues, particularly for applications in biological media, where the unique characteristics of ROMP provide distinct advantages over other polymerization strategies.

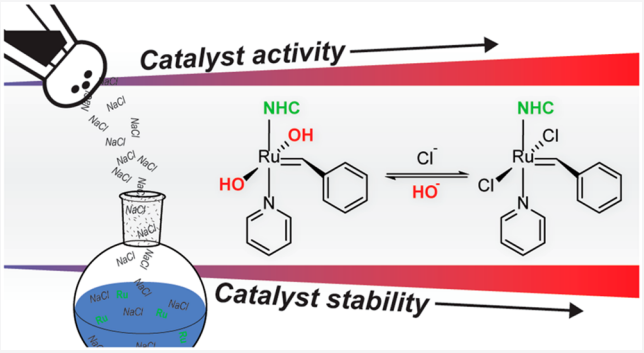

INTRODUCTION

Olefin metathesis has emerged as a powerful tool for the construction of C−C bonds, both in organic transformations of small molecules and the synthesis of polymers via ring-opening metathesis polymerization (ROMP).[1] As applications of this versatile technology continue to expand, the demand for increasingly active and robust metathesis catalysts has intensified, requiring a deeper understanding of the factors underlying catalyst performance and deactivation pathways under a variety of reaction conditions. Modern Ru-based catalysts containing *N*-heterocyclic carbene (NHC) ligands exhibit high functional group tolerance, and their robustness has recently been leveraged to carry out metathesis reactions in alcoholic or aqueous media.[2,3] Increasing interest in performing metathesis in H_2O, a green alternative solvent, has led to the optimization of cross-metathesis (CM) and ring-closing metathesis (RCM) reactions under aqueous conditions using water-soluble catalysts. In addition to reducing the environmental impact of these processes, it has further broadened the applications of aqueous olefin metathesis in biochemical research.[4−9] More recently, aqueous metathesis has been exploited to graft polymers from proteins in biological media,[10,11] realize molecular transformations within living cells,[12] and prepare polymeric nanoparticles via self-assembly methods such as ring-opening metathesis polymerization-induced self-assembly (ROMPISA)[13−17] and others.[18−20]

Despite these accomplishments, aqueous olefin metathesis remains challenging. Metathesis catalysts must be rendered water-soluble through ligand modification to achieve homogeneous reactions. Water-soluble Ru-NHC catalysts have been developed by the groups of Grubbs,[21−25] Grela,[26,27] Emrick,[28,29] and others,[30−33] that display charged/PEGylated NHC, phosphine, pyridine (Py), or styryl ether (Hoveyda-

Received: May 19, 2020
Published: July 16, 2020

https://dx.doi.org/10.1021/jacs.0c05499
J. Am. Chem. Soc. 2020, 142, 13878−13885

type) ligands. Although these efforts have simplified aqueous-phase metathesis chemistry, the impact of H_2O on the activity and stability of Ru-NHC catalysts remains largely unexplored. It is convenient to assume that the chemical structure of the metathesis-active species is consistent regardless of solvent; however, anomalous results reported in the literature and obtained in our lab,[13,22,29,34,35] including higher than expected polymer molecular weights, low monomer conversions, and slow polymerization kinetics compared with polymerizations in aprotic solvent, suggest that a different, less active, and less stable species could be present in alcoholic/aqueous solution.

Our lack of understanding of aqueous metathesis chemistry stems, in part, from the methodology typically employed to evaluate new water-soluble catalysts. Substrates used to probe the aqueous metathesis activity of these new catalysts are most often readily cyclized RCM targets or highly reactive CM substrates. In addition, high catalyst loadings (i.e., 5−10 mol %) are often employed in initial screenings, giving exaggeratedly high reaction conversions while masking issues of catalyst deactivation. Such artificial conditions do not reflect the complexity involved in RCM or CM of challenging substrates, reactions involving biomacromolecules, or the synthesis of high MW or multiblock polymers via ROMP.

Our group recently developed a two-step approach to carry out controlled ROMPISA in aqueous solution using Grubbs' third-generation catalyst, **G3**, which is commercially available.[13,14,17] Initiation of **G3** in a water-miscible solvent and polymerization of a few units of hydrophilic monomer was found to be sufficient to achieve catalyst solubilization in solvent mixtures containing high concentrations of H_2O (e.g., ≥ 90 v/v %). However, acidification of the reaction mixtures with HCl to ca. pH 2 was required to attain quantitative monomer conversions during chain-extension, limiting our capability to carry out polymerizations in the presence of sensitive biomolecules such as enzymes. Thus, it became important to understand the dependence of catalyst activity on acid to enable polymerization under neutral conditions. In this contribution, we investigate the influences of solution pH, catalyst loading, salt concentration, and other factors on the activity and stability of common metathesis catalysts in aqueous media using monomer conversion as the principal parameter of comparison. Chloride concentration, in particular, was found to play a pivotal role in both enhancing the rate of propagation and slowing the rate of catalyst decomposition, resulting in increased catalyst turnover and lifetime. These effects were consistent for both **G3** and the water-soluble catalyst AquaMet (**AM**), suggesting that chloride ion concentration is generally important for aqueous metathesis using Ru-based catalysts. In addition, we provide mechanistic insights into the nature of the active catalytic species in aqueous solution and demonstrate practical implications by preparing diblock copolymer nano-objects via ROMPISA.

RESULTS AND DISCUSSION

To better understand the relationship between solution pH and aqueous ROMP activity, we carried out screening studies at 1 mol % catalyst in mixed solutions (9:1 v/v H_2O/THF, 100 mM phosphate) with different pH values (pH 2−7). HCl was employed to adjust solution pH. Common metathesis catalysts **G3**, **AM**, and **G2** were selected for screening and **MPEG**, a water-soluble *exo*-norbornene derivative, was used as the monomer (Figure 1). After 2 h, the polymerizations were analyzed by ^{1}H NMR spectroscopy to determine monomer

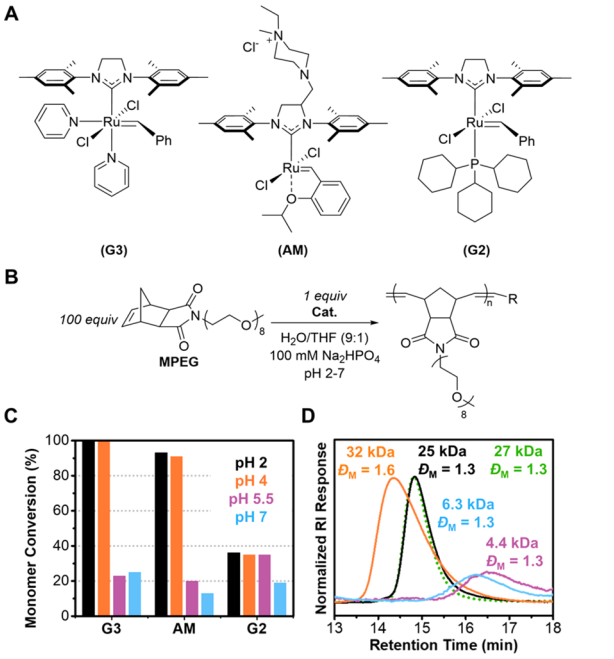

Figure 1. (A) Chemical structures of Ru-based metathesis catalysts used in initial ROMP screening. (B) Polymerization conditions employed for ROMP screening. (C) Monomer conversion under various conditions, as determined by ^{1}H NMR spectroscopy in methanol-d_4. (D) Conversion-normalized SEC RI traces (eluent: THF + 2 v/v% NEt_3) of polymers obtained via ROMP using **G3** at different pH values, or in THF (green, dotted trace).

conversion and size-exclusion chromatography (SEC) to calculate polymer number-average molecular weight (M_n) and dispersity ($Đ_M$), respectively. For comparison, an additional polymerization was conducted in pure organic solvent (THF) at the same monomer and catalyst concentrations. The results of this initial screening are shown in Figure 1 (additional results can be found in Table S1 and Figure S4).

It was evident from these data that pH (and thus acid concentration) had a dramatic impact on monomer conversion. In all cases, increasing the pH of the polymerization solutions resulted in decreased conversions. These data appear to oppose previous reports on aqueous ROMPISA using **AM**, where quantitative conversions and narrow molecular weight distributions were obtained at neutral pH.[16,36] However, these studies employed relatively higher initial catalyst concentrations than those used herein.[37] Increasing the solution pH from 2 to 4 also resulted in broader $Đ_M$ despite both polymerizations achieving quantitative conversion, indicating slower catalyst initiation and/or catalyst decomposition at pH 4. It was also surprising that monomer conversions when using **G2** were generally low regardless of pH. Fogg and co-workers showed that PCy_3 catalyzes Ru carbene decomposition in the presence of basic or donor compounds;[38,39] thus, we supposed that **G2** might decompose more rapidly in aqueous media relative to **G3** or **AM**.

We also evaluated different acid sources. HCl has been used almost exclusively as the Brønsted acid additive in previous studies on aqueous ROMP. We wondered if, in addition to H^+ concentration, the identity of the acid counterion was also important. Thus, additional screening polymerizations were carried out in pH 2 solution acidified with H_2SO_4 or H_3PO_4

https://dx.doi.org/10.1021/jacs.0c05499
J. Am. Chem. Soc. 2020, 142, 13878−13885

using **G3** as the catalyst under otherwise identical experimental conditions (Figure 2A and Figure S6A and Table S3).

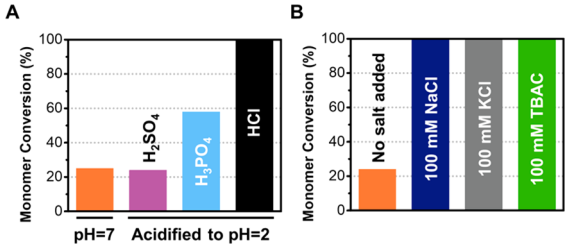

Figure 2. Monomer conversions obtained from additional screening polymerizations of **MPEG** using **G3** to evaluate different (A) acids or (B) salt additives, as determined by ^{1}H NMR spectroscopy in methanol-d_4.

In contrast to the polymerizations conducted with HCl, the use of H_2SO_4 or H_3PO_4 as the source of acid did not enable quantitative monomer conversions. Therefore, it was concluded that additional mechanistic complexity, related to the identity of the acid counterion (Cl^- in initial screening), was underlying the activity of the catalyst in aqueous conditions. The role of H^+ has been widely implicated as the primary determinant in aqueous metathetical activity, promoting ligand dissociation,[40−42] and protecting the catalysts from decomposition via nucleophilic addition,[38,43] or β-elimination,[39,44] pathways.[23,34] However, added salt has also been shown to increase RCM conversions in H_2O and has been suggested to improve control in aqueous dispersion ROMP.[45,46] Thus, the importance of the chloride ion was further considered by employing various salts as neutral sources of chloride ions instead of HCl. It was found that the addition of both organic (TBAC) or inorganic (NaCl or KCl) chloride salts at 100 mM to polymerizations of **MPEG** under neutral conditions in 9:1 v/v H_2O/THF had a profound effect, enabling quantitative monomer conversions (Figure 2B). Moreover, ROMP with TBAC yielded a polymer with M_n and $Đ_M$ values similar to those of the sample obtained via ROMP at pH 2 (Figure S6B).

The dependence of monomer conversion on the presence of chloride ions indicated that chloride ligand displacement, perhaps by water or hydroxide ions, was occurring at the Ru center in aqueous media, resulting in low catalyst turnover. The exchange of halide ligands with anionic compounds has been well documented in the literature.[47−51] Indeed, DFT calculations indicate that Cl^- dissociation from Ru-based complexes in polar solvents can compete with dissociation of so-called "labile" ligands such as PCy_3 and Py.[52] Moreover, Grubbs and co-workers identified that Cl^- dissociation and subsequent coordination of H_2O to Ru was a key step in the formation of high energy, unstable carbene intermediates, and the formation of such species could introduce alternative catalyst decomposition pathways in aqueous media.[53] In the case of chloride exchange in aqueous media, the formation of inactive and unstable Ru-$(OH)_n$ species could account for the observed decreases in monomer conversion. Ru-$(OH)_n$ complexes are ubiquitous,[54,55] but hydroxide-containing Ru carbene catalysts have only very recently been demonstrated to exist. Fogg and co-workers synthesized a Ru-$(OH)_n$ carbene complex, **HG2-$(OH)_2$**, by treating Hoveyda-Grubbs second-generation catalyst (**HG2**) with an excess of tetrabutylammonium hydroxide in mixed media containing THF and H_2O.[51] The resulting complex was shown to be completely inert to metathetical activity, attributed to reduced electron density on the Ru center via inductive withdrawal by the hydroxide ligands. It was also shown that **HG2-$(OH)_2$** was more susceptible to degradation than the native chloride complex. Thus, we supposed that chloride ligand displacement would be equally probable for other Ru carbene catalysts, such as **G3**, and that ligand exchange equilibria, involving both H^+ and Cl^-, explained the observed effects of the various acids and salts that were screened (Scheme 1).

Scheme 1. Roles of H^+ and Cl^- in Ru Complex Equilibria in Aqueous Media

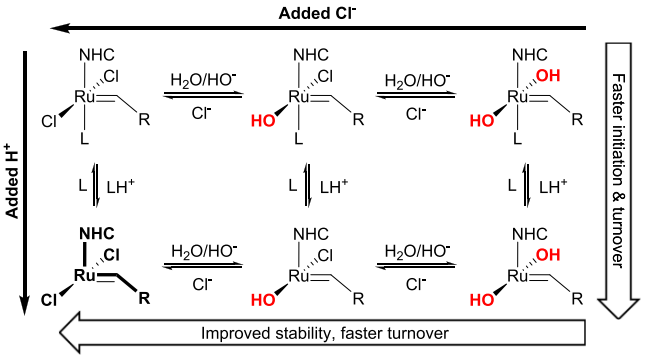

Importantly, we hypothesize that H^+ and Cl^- perform different roles in aqueous ROMP. The presence of Cl^- is fundamental to inhibiting chloride ligand exchange, which would result in the formation of metathesis inactive Ru-$(OH)_n$. Meanwhile, H^+ promotes fast catalyst initiation and turnover by protonation of pyridine ligands present on **G3**, thus facilitating the formation of the 14e$^-$ active species. Indeed, it was found that polymerization of **MPEG** in 100 mM chloride salts yielded broader $Đ_M$ than pH 2 HCl, indicating that initiation was slower in the absence of H^+. It should also be noted that pH 2 HCl enabled quantitative conversion despite containing only 10 mM Cl^-, which would appear to be insufficient if only the role of Cl^- was considered. This finding can be explained by considering the concentration of pyridine in solution, which has been shown to directly affect the rate of propagation.[40] The formation of noncoordinating pyridinium salts in the presence of HCl effectively decreased the concentration of pyridine in solution, thus enabling faster propagation kinetics that outcompete catalyst decomposition. The separate roles of H^+ and Cl^- in Ru complex equilibria are further corroborated in studies by Grubbs and co-workers whereby coordination of H_2O to Ru was found to be responsible for degenerative alkylidene H/D exchange.[53] Importantly, the rate of H/D exchange and thus coordination of H_2O was found to be inversely proportional to the concentration of NaCl. Conversely, the addition of Brønsted acid did not significantly influence the rate of H/D exchange, indicating that H^+ does not play a significant role in chloride ligand exchange despite decreasing the effective concentration of H_2O and HO^-.

Ligand exchange was corroborated in our system via kinetic analysis. Polymerizations of **MPEG** were conducted in 9:1 v/v H_2O/THF at neutral pH in the presence of different concentrations of TBAC as the chloride source (20−80 mM) using **G3** at 1 mol %. Aliquots of the polymerization solutions were sampled at regular intervals, quenched with ethyl vinyl ether (EVE), and analyzed by ^{1}H NMR spectros-

https://dx.doi.org/10.1021/jacs.0c05499
J. Am. Chem. Soc. 2020, 142, 13878−13885

copy to evaluate propagation kinetics. It should be noted that kinetic monitoring of polymerization in the absence of TBAC was not possible, as the polymerizations rapidly achieved their maximum conversions (ca. 25% in t = 1 min) and terminated, likely due to fast catalyst decomposition.

As shown in Figure 3 (and Figures S7–S12), TBAC concentration had a dramatic influence on both propagation rate and the final monomer conversion that was achieved in each trial, with the highest TBAC concentration leading to the fastest polymerization kinetics and highest monomer conversion. The polymerizations were pseudo-first order in monomer after an initial period of rapid conversion (ca. 2 min) that was attributed to fast turnover by the Ru–Cl_2 complex prior to its equilibration with the mono- and/or dihydroxide species (see the Supporting Information for further discussion). A linear relationship between chloride ion concentration and observed rate constant confirmed the incidence of ligand exchange acting coincidentally with catalyst turnover (Figure 3C). It should be noted that propagation kinetics were significantly slower in H_2O compared with kinetics in THF, regardless of TBAC loading. In addition, the dispersities of the resulting polymers generally decreased with increasing TBAC concentration (Figure 3D and Table S4), consistent with increased polymerization rate relative to catalyst deactivation (vide infra).

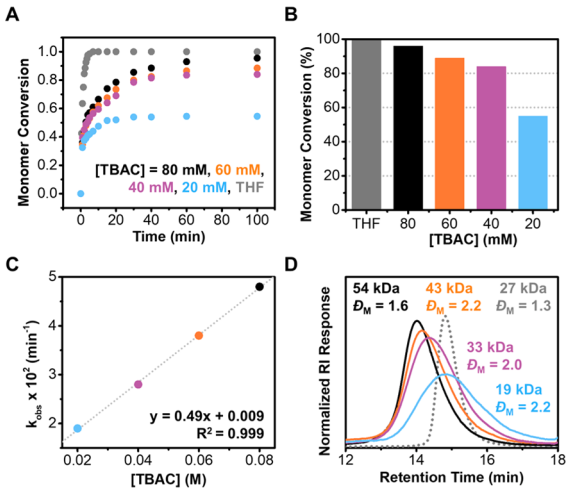

Figure 3. (A) Kinetics of ROMP targeting $DP_{P(MPEG)}$ = 100 in the presence of different TBAC concentrations using **G3** at 1 mol % in 9:1 v/v H_2O/THF at neutral pH. Monomer conversions were determined using ^1H NMR spectroscopy in methanol-d_4. The gray data series represents kinetics of a control polymerization in THF targeting the same $DP_{P(MPEG)}$. (B) ROMP monomer conversion as a function of TBAC concentration obtained from the kinetic data. (C) Plot of k_{obs} vs. TBAC concentration generated using the kinetic data in (A). (D) Conversion-normalized SEC RI traces (eluent: THF + 2 v/v% NEt_3) of the final time points of the kinetic experiments and a polymerization in THF (gray dotted trace). The colors of the data in C and D correspond to the legend in A.

In addition to polymerization kinetics, we also investigated the stability of **G3** and **AM** in H_2O in the presence or absence of TBAC. The precatalysts were incubated in 9:1 v/v H_2O/THF mixtures containing either 30 mM TBAC or no TBAC at neutral pH, and their decomposition was monitored in situ by measuring the change in absorbance every 90 s for 1 h, a typical time frame in which aqueous ROMP reaches full or final conversion. As shown in Figure 4, the absorbance at λ_{max} = 343 nm, corresponding to the metal–ligand charge transfer (MLCT) band associated with the Ru-benzylidene,[45,56] decreased over the course of the experiments, signifying loss of the carbene moiety and thus catalyst decomposition. These trends were even more significant for **AM**, which did not decompose appreciably in neutral aqueous media containing 30 mM TBAC within the time frame of the experiment (Figure S13). The origin of the change in apparent decomposition order is currently unknown but has been observed elsewhere.[45] Although these data seem to imply that **AM** is more suitable than **G3** for ROMP in aqueous media, the relative stabilities of the **G3** and **AM** precatalyst species are not directly related to the stability of their respective propagating alkylidenes, which we expect would be similar based on their similar structures.

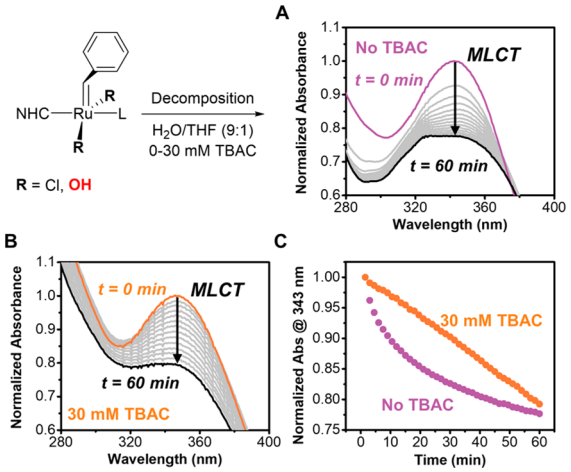

Figure 4. (A) Catalyst decomposition in neutral aqueous media leads to loss of the carbene and a decrease in absorbance of the MLCT band. Shown are the UV–vis spectra for **G3**, collected every 90 s over 1 h, in the (A) absence or (B) presence of 30 mM TBAC. (C) Change in MLCT band absorbance over time depending on incubation conditions.

We next sought to identify the formation of Ru-$(OH)_n$ species in situ. Upon addition of 2 equiv. of NaOH to **G3**, a shift in the benzylidene proton from 16.0 to 15.3 ppm in the ^1H NMR spectrum was observed (Figure S16A), consistent with recent results from Fogg, where a similar upfield shift in the benzylidene proton was observed for their hydroxide catalyst **HG2-(OH)$_2$** relative to **HG2**.[51] In addition, new peaks emerged in the 6–7 ppm region that were attributed to changes in the environments of the mesityl protons in response to ligand exchange (there was no change in overall integration in this region). Benzaldehyde and benzyl alcohol were also detected as byproducts of catalyst decomposition, both of which were presumably derived from the styrenic benzylidene ligand.[57] It should also be noted that the formation of Ru hydride species could also be detected after incubation of **G3** with NaOH for 2 h (Figure S15), suggesting a probable mechanism of decomposition for the Ru-$(OH)_n$ species.[47,58,59] The effect of chloride ligand exchange on complex absorption was also investigated. Upon dissolution of **G3** into 9:1 v/v H_2O/THF, a MLCT band was apparent in the UV–vis spectrum with λ_{max} = 343 nm. Addition of increasing amounts of TBAC resulted in a proportional red shift of the MLCT band (Figure S16B). These findings indicate that rapid ligand exchange was occurring during mixing of the **G3** stock solution (in THF) with H_2O solutions containing varying amounts of TBAC. These data are strongly suggestive of the in situ

https://dx.doi.org/10.1021/jacs.0c05499
J. Am. Chem. Soc. 2020, 142, 13878–13885

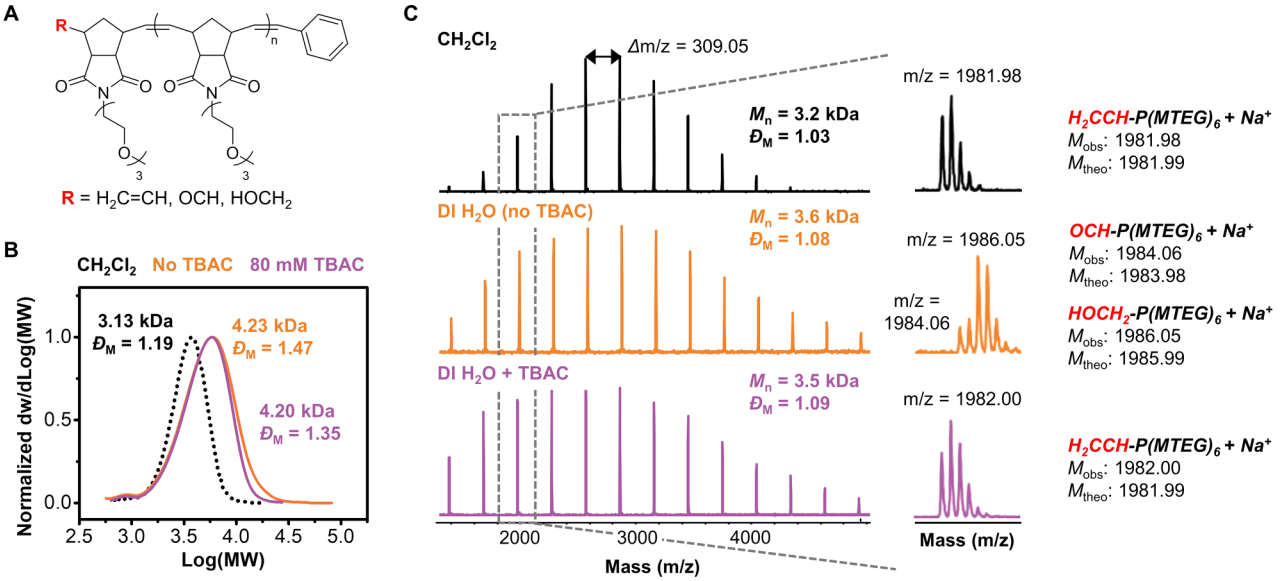

Figure 5. (A) Observed ω-end groups for P(**MTEG**)$_{10}$ homopolymers synthesized under various conditions. (B) Normalized SEC MW distributions (eluent: THF + 2 v/v% NEt_3, PS standards) of the P(**MTEG**)$_{10}$ homopolymers. (C) MALDI-ToF mass spectra of the P(**MTEG**)$_{10}$ homopolymers prepared under different conditions. The enlarged regions show the isotopic distributions for the $DP_{P(MTEG)} = 6$ species highlighted by the dashed square. DCTB was used as the matrix and CF_3COONa as the cation source.

formation of **G3**-$(OH)_n$; however, it should be noted that attempts to isolate this complex were unsuccessful.

We also considered that decomposition during ROMP could influence polymer microstructure, in particular the nature of the ω-end group associated with the Ru center. Typically, terminal alkene end groups are expected for polymers prepared by ROMP and terminated with vinyl ethers such as EVE, resulting in the formation of a stable Fisher carbene and liberation of a methylene end-functionalized polymer chain. However, breakdown of the catalyst prior to intentional termination would preclude the formation of such end groups due to loss of the carbene moiety.[38,39,43,44,60,61] To evaluate the influence of catalyst decomposition on polymer end groups, we carried out a series of polymerizations in 9:1 v/v H_2O/THF in the presence or absence of 80 mM TBAC or in CH_2Cl_2 as a positive control. A DP of 10 was targeted in these polymerizations using a monodisperse triethylene glycol monomethyl ether norbornene monomer (**MTEG**) to facilitate polymer characterization by matrix-assisted laser desorption/ionization time-of-flight (MALDI-ToF) mass spectrometry and ^{1}H NMR spectroscopy.

As shown in Figure 5C (and in the ^{1}H NMR spectrum in Figure S18), the sample of P(**MTEG**)$_{10}$ prepared in CH_2Cl_2 that was quenched with EVE possessed the expected α-phenyl and ω-alkene end groups (M_{obs} = 1981.98, M_{theo} = 1981.99, $\Delta m/z$ = 0.01). In contrast, the terminal alkene end group was completely absent from P(**MTEG**)$_{10}$ synthesized in aqueous media without TBAC. Instead, the predominate ω-end group species for this sample were terminal aldehydes (M_{obs} = 1984.06, M_{theo} = 1983.98, $\Delta m/z$ = 0.08) and alcohols (M_{obs} = 1984.06, M_{theo} = 1985.99, $\Delta m/z$ = 0.06), both of which were also present in the ^{1}H NMR spectrum shown in Figure S18. Although these two species have similar molecular formulas, the enlarged regions in Figure 5C show that their isotopic distributions appear to be different. This difference is attributed to the intensity contribution of the M+3 peak of aldehyde-terminated isotopic distribution (M_{obs} = 1986.05) to the M+1 peak of the alcohol-terminated species (M_{obs} = 1986.05). The presence of aldehyde and alcohol end groups indicated that the catalyst had decomposed prior to reaction with EVE,[62] resulting in the incorporation of oxygen into the polymer chain end. Importantly, the presence of 80 mM TBAC during aqueous ROMP was sufficient to prevent catalyst decomposition over the time frame of polymerization, thus allowing for the formation of the expected alkene ω-end group upon quenching of the catalyst with EVE (M_{obs} = 1982.00, M_{theo} = 1981.99 $\Delta m/z$ = 0.01). These subtle differences in polymer samples arising from slight changes in ROMP procedure were not apparent in the SEC data (Figure 5B), where the traces appeared similar for the samples prepared in aqueous media in the presence/absence of TBAC.

To better understand the scope of aqueous ROMP at neutral pH, we synthesized a P(**MPEG**)$_{20}$ homopolymer and attempted chain-extension with two sequential additions of 20 equiv. **MPEG** (Figure S19 and Table S6). Despite the chain extensions achieving quantitative conversion, the dispersities of the resultant polymers indicated that the polymerization was not well-controlled when initiated in pH-neutral water with 100 mM NaCl. We hypothesized that the broad dispersities could arise due to slow catalyst initiation in the absence of H^+. Furthermore, the high concentrations of **G3** employed to achieve DP = 20 (i.e., 5 mol %) resulted in catalyst precipitation and thus heterogeneous polymerization, making control over molecular weight challenging.

We next attempted ROMPISA using our previously reported two-step procedure (Figure 6A). Our efforts to perform ROMPISA in the absence of HCl were unsuccessful, which we attribute to the formation of metathesis inactive Ru-$(OH)_n$ species and/or catalyst decomposition prior to nanoparticle nucleation. In this instance, DI H_2O containing 100 mM NaCl was used as the solvent in lieu of acidic phosphate buffer (pH 2). To circumvent issues of catalyst solubility and slow catalyst initiation in H_2O, a short block of P(**MPEG**) ($DP_{P(MPEG)}$ = 10) was first prepared in THF. This macroinitiator was then added to *exo*-norbornene methyoxyethylene imide (**MMEG**) dissolved in 100 mM NaCl solution (neutral pH). Different

https://dx.doi.org/10.1021/jacs.0c05499
J. Am. Chem. Soc. 2020, 142, 13878−13885

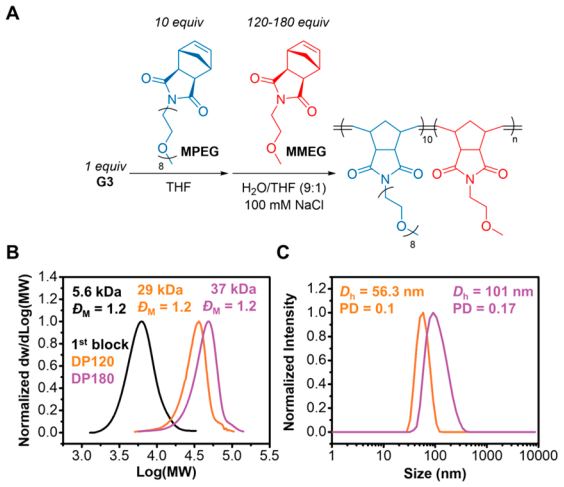

Figure 6. (A) Synthesis of P(**MPEG**)$_{10}$-*b*-P(**MMEG**)$_n$ diblock copolymer nano-objects by ROMPISA at neutral pH w/100 mM NaCl. (B) Normalized SEC MW distributions (eluent: THF + 2 v/v% NEt_3, PS standards) of the P(**MPEG**)$_{10}$ macroinitiator and P(**MPEG**)$_{10}$-*b*-P(**MMEG**)$_n$ diblock copolymers. (C) Intensity-weighted DLS traces of diblock copolymer nano-objects prepared by aqueous ROMPISA at neutral pH.

DPs of this core-forming P(**MMEG**) block were targeted ($DP_{P(MMEG)}$ = 120 and 180) to evaluate polymerization control. As shown in Figure 6B and Table S7, P(**MPEG**)$_{10}$-*b*-P(**MMEG**)$_n$ diblock copolymers were obtained with low dispersities and M_n that agreed with expected values. Quantitative monomer conversions were achieved in all cases. In addition, polymeric nano-objects were readily obtained, with hydrodynamic diameters that scaled from ca. 60−100 nm proportionally to $DP_{P(MMEG)}$, suggesting the formation of progressively larger nano-objects (Figure 6C and Figure S20).

CONCLUSIONS

The excellent activity of aqueous metathesis catalysts at low solution pH has been previously ascribed (for select complexes) to the involvement of H^+ in ligand dissociation and/or neutralization of HO^-. However, we have shown, using screening and kinetic experiments, that aqueous ROMP is significantly more sensitive to the concentration of Cl^- than the concentration of H^+, and this sensitivity stems from displacement of chloride ligands by hydroxide or H_2O at the Ru center. We also demonstrated through in situ experiments that the resulting Ru-$(OH)_n$ complexes decompose rapidly via carbene loss and exhibit limited to no metathetical activity. Addition of chloride negated Ru-$(OH)_n$ formation during aqueous ROMP and enabled quantitative monomer conversion and increased polymerization control, facilitating the controlled synthesis of diblock copolymers via ROMPISA in solutions with high water concentrations, neutral pH values, and moderate-to-low catalyst loadings. Catalyst decomposition was also found to have a significant impact on polymer microstructure, resulting in the formation of alcohol and aldehyde polymer end groups in the absence of Cl^-. The formation of such end groups has significant ramifications for aqueous ROMP including the syntheses of end-functionalized polymers and block copolymers. The capability to perform aqueous ROMP at neutral pH represents a significant improvement upon existing systems that rely on acidic conditions to enable productive metathetical activity. We anticipate that these findings will enable new applications of ROMP in H_2O, particularly for the synthesis of polymers, the formulation of polymeric nanoparticles, and the modification of biomacromolecules under biologically relevant conditions.

ASSOCIATED CONTENT

Supporting Information

The Supporting Information is available free of charge at https://pubs.acs.org/doi/10.1021/jacs.0c05499.

Materials and characterization techniques, synthetic procedures, supplementary NMR and SEC analysis data of polymers, kinetic plots, and additional UV−vis, MALDI-ToF, and DLS analysis data (PDF)

AUTHOR INFORMATION

Corresponding Authors

Jeffrey C. Foster − *School of Chemistry, University of Birmingham, Birmingham B15 2TT, United Kingdom*; Email: fosterjc@bham.ac.uk

Scott M. Grayson − *Department of Chemistry, Tulane University, New Orleans, Louisiana 70118, United States*; orcid.org/0000-0001-6345-8762; Email: sgrayson@tulane.edu

Rachel K. O'Reilly − *School of Chemistry, University of Birmingham, Birmingham B15 2TT, United Kingdom*; orcid.org/0000-0002-1043-7172; Email: r.oreilly@bham.ac.uk

Authors

Marcus C. Grocott − *School of Chemistry, University of Birmingham, Birmingham B15 2TT, United Kingdom*

Lucy A. Arkinstall − *School of Chemistry, University of Birmingham, Birmingham B15 2TT, United Kingdom*

Spyridon Varlas − *School of Chemistry, University of Birmingham, Birmingham B15 2TT, United Kingdom*

McKenna J. Redding − *Department of Chemistry, Tulane University, New Orleans, Louisiana 70118, United States*

Complete contact information is available at: https://pubs.acs.org/10.1021/jacs.0c05499

Author Contributions

†J.C.F. and M.C.G. contributed equally.

Notes

The authors declare no competing financial interest.

ACKNOWLEDGMENTS

This work was supported by the ERC (Grant 615142), EPSRC, and the University of Birmingham.

REFERENCES

(1) Ogba, O. M.; Warner, N. C.; O'Leary, D. J.; Grubbs, R. H. Recent advances in ruthenium-based olefin metathesis. *Chem. Soc. Rev.* **2018**, *47*, 4510−4544.

(2) Tomasek, J.; Schatz, J. Olefin metathesis in aqueous media. *Green Chem.* **2013**, *15*, 2317−2338.

(3) Lipshut, B. H.; Ghoral, S.Olefin Metathesis in Water and Aqueous Media. In *Olefin Metathesis: Theory and Practice*; Grela, K., Ed.; Wiley, 2015; Chapter 21, pp 515−521.

(4) Lin, Y. A.; Davis, B. G.Vignette: Extending the Application of Metathesis in Chemical Biology—The Development of Site-Selective Peptide and Protein Modifications. In *Handbook of Metathesis*;

Grubbs, R. H., Wenel, A. G., O'Leary, D. J., Khosravi, E., Eds.; Wiley, 2015; Chapter 3, pp 295−309.
(5) Masuda, S.; Tsuda, S.; Yoshiya, T. Ring-closing metathesis of unprotected peptides in water. *Org. Biomol. Chem.* **2018**, *16*, 9364−9367.
(6) Zhao, J.; Kajetanowicz, A.; Ward, T. R. Carbonic anhydrase II as host protein for the creation of a biocompatible artificial metathesase. *Org. Biomol. Chem.* **2015**, *13*, 5652−5655.
(7) Lin, Y. A.; Chalker, J. M.; Floyd, N.; Bernardes, G. J. L.; Davis, B. G. Allyl Sulfides Are Privileged Substrates in Aqueous Cross-Metathesis: Application to Site-Selective Protein Modification. *J. Am. Chem. Soc.* **2008**, *130*, 9642−9643.
(8) Lu, X.; Fan, L.; Phelps, C. B.; Davie, C. P.; Donahue, C. P. Ruthenium Promoted On-DNA Ring-Closing Metathesis and Cross-Metathesis. *Bioconjugate Chem.* **2017**, *28*, 1625−1629.
(9) Lin, Y. A.; Boutureira, O.; Lercher, L.; Bhushan, B.; Paton, R. S.; Davis, B. G. Rapid Cross-Metathesis for Reversible Protein Modifications via Chemical Access to Se-Allyl-selenocysteine in Proteins. *J. Am. Chem. Soc.* **2013**, *135*, 12156−12159.
(10) Isarov, S. A.; Pokorski, J. K. Protein ROMP: Aqueous Graft-from Ring-Opening Metathesis Polymerization. *ACS Macro Lett.* **2015**, *4*, 969−973.
(11) Lee, P. W.; Isarov, S. A.; Wallat, J. D.; Molugu, S. K.; Shukla, S.; Sun, J. E. P.; Zhang, J.; Zheng, Y.; Lucius Dougherty, M.; Konkolewicz, D.; Stewart, P. L.; Steinmetz, N. F.; Hore, M. J. A.; Pokorski, J. K. Polymer Structure and Conformation Alter the Antigenicity of Virus-like Particle−Polymer Conjugates. *J. Am. Chem. Soc.* **2017**, *139*, 3312−3315.
(12) Jeschek, M.; Reuter, R.; Heinisch, T.; Trindler, C.; Klehr, J.; Panke, S.; Ward, T. R. Directed evolution of artificial metalloenzymes for in vivo metathesis. *Nature* **2016**, *537*, 661−665.
(13) Foster, J. C.; Varlas, S.; Blackman, L. D.; Arkinstall, L. A.; O'Reilly, R. K. Ring-Opening Metathesis Polymerization in Aqueous Media Using a Macroinitiator Approach. *Angew. Chem., Int. Ed.* **2018**, *57*, 10672−10676.
(14) Varlas, S.; Foster, J. C.; Arkinstall, L. A.; Jones, J. R.; Keogh, R.; Mathers, R. T.; O'Reilly, R. K. Predicting Monomers for Use in Aqueous Ring-Opening Metathesis Polymerization-Induced Self-Assembly. *ACS Macro Lett.* **2019**, *8*, 466−472.
(15) Varlas, S.; Foster, J. C.; O'Reilly, R. K. Ring-opening metathesis polymerization-induced self-assembly (ROMPISA). *Chem. Commun.* **2019**, *55*, 9066−9071.
(16) Wright, D. B.; Touve, M. A.; Thompson, M. P.; Gianneschi, N. C. Aqueous-Phase Ring-Opening Metathesis Polymerization-Induced Self-Assembly. *ACS Macro Lett.* **2018**, *7*, 401−405.
(17) Varlas, S.; Keogh, R.; Xie, Y.; Horswell, S. L.; Foster, J. C.; O'Reilly, R. K. Polymerization-Induced Polymersome Fusion. *J. Am. Chem. Soc.* **2019**, *141*, 20234−20248.
(18) Chen, Z.; Mercer, J. A. M.; Zhu, X.; Romaniuk, J. A. H.; Pfattner, R.; Cegelski, L.; Martinez, T. J.; Burns, N. Z.; Xia, Y. Mechanochemical unzipping of insulating polyladderene to semiconducting polyacetylene. *Science* **2017**, *357*, 475−479.
(19) Yoon, K.-Y.; Lee, I.-H.; Kim, K. O.; Jang, J.; Lee, E.; Choi, T.-L. One-Pot in Situ Fabrication of Stable Nanocaterpillars Directly from Polyacetylene Diblock Copolymers Synthesized by Mild Ring-Opening Metathesis Polymerization. *J. Am. Chem. Soc.* **2012**, *134*, 14291−14294.
(20) Shin, S.; Gu, M.-L.; Yu, C.-Y.; Jeon, J.; Lee, E.; Choi, T.-L. Polymer Self-Assembly into Unique Fractal Nanostructures in Solution by a One-Shot Synthetic Procedure. *J. Am. Chem. Soc.* **2018**, *140*, 475−482.
(21) Mohr, B.; Lynn, D. M.; Grubbs, R. H. Synthesis of Water-Soluble, Aliphatic Phosphines and Their Application to Well-Defined Ruthenium Olefin Metathesis Catalysts. *Organometallics* **1996**, *15*, 4317−4325.
(22) Lynn, D. M.; Mohr, B.; Grubbs, R. H. Living Ring-Opening Metathesis Polymerization in Water. *J. Am. Chem. Soc.* **1998**, *120*, 1627−1628.
(23) Lynn, D. M.; Kanaoka, S.; Grubbs, R. H. Living Ring-Opening Metathesis Polymerization in Aqueous Media Catalyzed by Well-Defined Ruthenium Carbene Complexes. *J. Am. Chem. Soc.* **1996**, *118*, 784−790.
(24) Hong, S. H.; Grubbs, R. H. Highly Active Water-Soluble Olefin Metathesis Catalyst. *J. Am. Chem. Soc.* **2006**, *128*, 3508−3509.
(25) Jordan, J. P.; Grubbs, R. H. Small-Molecule N-Heterocyclic-Carbene-Containing Olefin-Metathesis Catalysts for Use in Water. *Angew. Chem., Int. Ed.* **2007**, *46*, 5152−5155.
(26) Gułajski, Ł.; Michrowska, A.; Bujok, R.; Grela, K. New tunable catalysts for olefin metathesis: Controlling the initiation through electronic factors. *J. Mol. Catal. A: Chem.* **2006**, *254*, 118−123.
(27) Skowerski, K.; Szczepaniak, G.; Wierzbicka, C.; Gułajski, Ł.; Bieniek, M.; Grela, K. Highly active catalysts for olefin metathesis in water. *Catal. Sci. Technol.* **2012**, *2*, 2424−2427.
(28) Breitenkamp, K.; Emrick, T. Amphiphilic ruthenium benzylidene metathesis catalyst with PEG-substituted pyridine ligands. *J. Polym. Sci., Part A: Polym. Chem.* **2005**, *43*, 5715−5721.
(29) Samanta, D.; Kratz, K.; Zhang, X.; Emrick, T. A Synthesis of PEG- and Phosphorylcholine-Substituted Pyridines To Afford Water-Soluble Ruthenium Benzylidene Metathesis Catalysts. *Macromolecules* **2008**, *41*, 530−532.
(30) Dunbar, M. A.; Balof, S. L.; Roberts, A. N.; Valente, E. J.; Schanz, H.-J. pH-Responsive Ruthenium-Based Olefin Metathesis Catalysts: Controlled Ring-Opening Metathesis Polymerization in Alcoholic and Aqueous Media upon Acid Addition. *Organometallics* **2011**, *30*, 199−203.
(31) Allaert, B.; Dieltiens, N.; Ledoux, N.; Vercaemst, C.; Van Der Voort, P.; Stevens, C. V.; Linden, A.; Verpoort, F. Synthesis and activity for ROMP of bidentate Schiff base substituted second generation Grubbs catalysts. *J. Mol. Catal. A: Chem.* **2006**, *260*, 221−226.
(32) Binder, J. B.; Guzei, I. A.; Raines, R. T. Salicylaldimine Ruthenium Alkylidene Complexes: Metathesis Catalysts Tuned for Protic Solvents. *Adv. Synth. Catal.* **2007**, *349*, 395−404.
(33) Yao, Q. A Soluble Polymer-Bound Ruthenium Carbene Complex: A Robust and Reusable Catalyst for Ring-Closing Olefin Metathesis. *Angew. Chem., Int. Ed.* **2000**, *39*, 3896−3898.
(34) Gallivan, J. P.; Jordan, J. P.; Grubbs, R. H. A neutral, water-soluble olefin metathesis catalyst based on an N-heterocyclic carbene ligand. *Tetrahedron Lett.* **2005**, *46*, 2577−2580.
(35) Takashima, Y.; Uramatsu, K.; Jomori, D.; Harima, A.; Otsubo, M.; Yamaguchi, H.; Harada, A. Ring-Opening Metathesis Polymerization by a Ru Phosphine Derivative of Cyclodextrin in Water. *ACS Macro Lett.* **2013**, *2*, 384−387.
(36) Wright, D. B.; Proetto, M. T.; Touve, M. A.; Gianneschi, N. C. Ring-opening metathesis polymerization-induced self-assembly (ROMPISA) of a cisplatin analogue for high drug-loaded nanoparticles. *Polym. Chem.* **2019**, *10*, 2996−3000.
(37) We attempted to replicate literature conditions by conducting ROMP using AM at 10 mol % and were able to achieve a similar outcome to previous reports (Table S2 and Figure S5). Decreasing the AM loading below 10 mol % resulted in a dramatic decrease in monomer conversion.
(38) McClennan, W. L.; Rufh, S. A.; Lummiss, J. A. M.; Fogg, D. E. A General Decomposition Pathway for Phosphine-Stabilized Metathesis Catalysts: Lewis Donors Accelerate Methylidene Abstraction. *J. Am. Chem. Soc.* **2016**, *138*, 14668−14677.
(39) Bailey, G. A.; Lummiss, J. A. M.; Foscato, M.; Occhipinti, G.; McDonald, R.; Jensen, V. R.; Fogg, D. E. Decomposition of Olefin Metathesis Catalysts by Brønsted Base: Metallacyclobutane Deprotonation as a Primary Deactivating Event. *J. Am. Chem. Soc.* **2017**, *139*, 16446−16449.
(40) Walsh, D. J.; Lau, S. H.; Hyatt, M. G.; Guironnet, D. Kinetic Study of Living Ring-Opening Metathesis Polymerization with Third-Generation Grubbs Catalysts. *J. Am. Chem. Soc.* **2017**, *139*, 13644−13647.

https://dx.doi.org/10.1021/jacs.0c05499
J. Am. Chem. Soc. 2020, 142, 13878−13885

(41) Bielawski, C. W.; Grubbs, R. H. Increasing the Initiation Efficiency of Ruthenium-Based Ring-Opening Metathesis Initiators: Effect of Excess Phosphine. *Macromolecules* **2001**, *34*, 8838−8840.
(42) P'Poo, S. J.; Schanz, H.-J. Reversible Inhibition/Activation of Olefin Metathesis: A Kinetic Investigation of ROMP and RCM Reactions with Grubbs' Catalyst. *J. Am. Chem. Soc.* **2007**, *129*, 14200−14212.
(43) Lummiss, J. A. M.; Ireland, B. J.; Sommers, J. M.; Fogg, D. E. Amine-Mediated Degradation in Olefin Metathesis Reactions that Employ the Second-Generation Grubbs Catalyst. *ChemCatChem* **2014**, *6*, 459−463.
(44) Ireland, B. J.; Dobigny, B. T.; Fogg, D. E. Decomposition of a Phosphine-Free Metathesis Catalyst by Amines and Other Bronsted Bases: Metallacyclobutane Deprotonation as a Major Deactivation Pathway. *ACS Catal.* **2015**, *5*, 4690−4698.
(45) Matsuo, T.; Yoshida, T.; Fujii, A.; Kawahara, K.; Hirota, S. Effect of Added Salt on Ring-Closing Metathesis Catalyzed by a Water-Soluble Hoveyda−Grubbs Type Complex To Form N-Containing Heterocycles in Aqueous Media. *Organometallics* **2013**, *32*, 5313−5319.
(46) Mingotaud, A.-F.; Mingotaud, C.; Moussa, W. Characterization of the micellar ring opening metathesis polymerization in water of a norbornene derivative initiated by Hoveyda-Grubbs' catalyst. *J. Polym. Sci., Part A: Polym. Chem.* **2008**, *46*, 2833−2844.
(47) Dinger, M. B.; Mol, J. C. Degradation of the First-Generation Grubbs Metathesis Catalyst with Primary Alcohols, Water, and Oxygen. Formation and Catalytic Activity of Ruthenium(II) Monocarbonyl Species. *Organometallics* **2003**, *22*, 1089−1095.
(48) Banti, D.; Mol, J. C. Degradation of the ruthenium-based metathesis catalyst $[RuCl_2(CHPh)(H_2IPr)(PCy_3)]$ with primary alcohols. *J. Organomet. Chem.* **2004**, *689*, 3113−3116.
(49) Tanaka, K.; Böhm, V. P. W.; Chadwick, D.; Roeper, M.; Braddock, D. C. Anionic Ligand Exchange in Hoveyda−Grubbs Ruthenium(II) Benzylidenes. *Organometallics* **2006**, *25*, 5696−5698.
(50) Lynn, D. M.; Grubbs, R. H. Novel Reactivity of Ruthenium Alkylidenes in Protic Solvents: Degenerate Alkylidene Proton Exchange. *J. Am. Chem. Soc.* **2001**, *123*, 3187−3193.
(51) Goudreault, A. Y.; Walden, D. M.; Nascimento, D. L.; Botti, A. G.; Steinmann, S. N.; Michel, C.; Fogg, D. E. Hydroxide-Induced Degradation of Olefin Metathesis Catalysts: A Challenge for Metathesis in Alkaline Media. *ACS Catal.* **2020**, *10*, 3838−3843.
(52) Falivene, L.; Poater, A.; Cazin, C. S. J.; Slugovc, C.; Cavallo, L. Energetics of the ruthenium−halide bond in olefin metathesis (pre)catalysts. *Dalton Trans.* **2013**, *42*, 7312−7317.
(53) Lynn, D. M.; Grubbs, R. H. Novel Reactivity of Ruthenium Alkylidenes in Protic Solvents: Degenerate Alkylidene Proton Exchange. *J. Am. Chem. Soc.* **2001**, *123*, 3187−3193.
(54) Nelson, D. J.; Nolan, S. P. Hydroxide complexes of the late transition metals: Organometallic chemistry and catalysis. *Coord. Chem. Rev.* **2017**, *353*, 278−294.
(55) Roesky, H. W.; Singh, S.; Yusuff, K. K. M.; Maguire, J. A.; Hosmane, N. S. Organometallic Hydroxides of Transition Elements. *Chem. Rev.* **2006**, *106*, 3813−3843.
(56) Sanford, M. S.; Love, J. A.; Grubbs, R. H. Mechanism and Activity of Ruthenium Olefin Metathesis Catalysts. *J. Am. Chem. Soc.* **2001**, *123*, 6543−6554.
(57) Forcina, V.; García-Domínguez, A.; Lloyd-Jones, G. C. Kinetics of initiation of the third generation Grubbs metathesis catalyst: convergent associative and dissociative pathways. *Faraday Discuss.* **2019**, *220*, 179−195.
(58) Manzini, S.; Fernández-Salas, J. A.; Nolan, S. P. From a Decomposition Product to an Efficient and Versatile Catalyst: The $[Ru(\eta_5\text{-indenyl})(PPh_3)_2Cl]$ Story. *Acc. Chem. Res.* **2014**, *47*, 3089−3101.
(59) Beach, N. J.; Lummiss, J. A. M.; Bates, J. M.; Fogg, D. E. Reactions of Grubbs Catalysts with Excess Methoxide: Formation of Novel Methoxyhydride Complexes. *Organometallics* **2012**, *31*, 2349−2356.
(60) Nelson, D. J.; Manzini, S.; Urbina-Blanco, C. A.; Nolan, S. P. Key processes in ruthenium-catalysed olefin metathesis. *Chem. Commun.* **2014**, *50*, 10355−10375.
(61) Bailey, G. A.; Foscato, M.; Higman, C. S.; Day, C. S.; Jensen, V. R.; Fogg, D. E. Bimolecular Coupling as a Vector for Decomposition of Fast-Initiating Olefin Metathesis Catalysts. *J. Am. Chem. Soc.* **2018**, *140*, 6931−6944.
(62) Coalter, I. I. I. J. N.; Bollinger, J. C.; Eisenstein, O.; Caulton, K. G. R-Group reversal of isomer stability for $RuH(X)L_2(CCHR)$s. $Ru(X)L_2(CCH_2R)$: access to four-coordinate ruthenium carbenes and carbynes. *New J. Chem.* **2000**, *24*, 925−927.

https://dx.doi.org/10.1021/jacs.0c05499
J. Am. Chem. Soc. 2020, 142, 13878−13885